

# Recent Advances in Charge Transport in Random Organic Solids: The Case of Conjugated Polymers and Discotic Liquid Crystals

D. Hertel,<sup>▲</sup> A. Ochse, V. I. Arkhipov, and H. Bässler

*Institut für Physikalische Chemie und Zentrum für Materialwissenschaften, Philipps-Universität Marburg, D-35032 Marburg*

The purpose of the present work is to delineate similarities as well as differences concerning the charge transporting properties of  $\pi$ -conjugated polymers as well as of discotic liquid crystals. Materials investigated are a (i) ladder-type poly-paraphenylene (LPPP), (ii) a member of the phenylenevinylene family, and (iii) several asymmetrically substituted triphenylenes. The disorder formalism explains the field and temperature dependence of the mobility adequately provided that the disorder, which is controlled by the sample topology and random dipolar electric fields, is sufficiently large. Differences are noted in highly ordered LPPP and in symmetric discotic crystals. It is conjectured that finite size effects in the case of LPPP and dynamic effects in the liquid crystals overcompensate the effect of energetic disorder.

Journal of Imaging Science and Technology 43: 220–227 (1999)

## Introduction

The disorder formalism has turned out to be a powerful tool to rationalize charge carrier motion in random organic solids.<sup>1–3</sup> The elementary event can be described by either a redox process or a hopping process, depending upon the terminology of either chemists or physicists, among chemically identical but physically different moieties, such as molecules or sub-units of a polymer. Structural disorder in a glassy system implies that their self-energies, for instance the van der Waals energies of molecular anions or cations in a polarizable medium, are distributed, as are the transfer integrals controlling charge or excitation exchange among the moieties. Unambiguous signatures are the inhomogeneous line widths in optical absorption or fluorescence spectra,<sup>4</sup> the broadening of diffraction features of electron micrographs of a molecular glass<sup>5</sup> or the distribution of intrinsic localized charge states in a polymer.<sup>6</sup> It is obvious that the roughness of the energy landscape in which charge carriers migrate has to depend on the shape of the molecules. If they carry polar functionalities their interaction energy will vary more strongly upon molecular displacement than apolar and more spherical molecules because the variations of the local electric field are larger.

A microscopic picture of charge carrier hopping in a random organic system was developed both via Monte Carlo (MC) simulations<sup>7</sup> and analytic effective medium theory.<sup>8</sup> One of its essential features is relaxation.<sup>9</sup> Upon generating an ensemble of charge carriers by a light flash the charge carrier tends to settle in the tail states

of the distribution of the hopping sites. Therefore transport must slow down in time and the equilibrium energy to which the ensemble relaxes must decrease as the temperature decreases. For this reason activation energy for hopping must increase at lower temperatures and transport must become dispersive.

There is abundant evidence that the above-mentioned concept is able to recover to basic experimental observations related to charge transport in organic glasses or molecularly doped polymers such as

- (i) the  $\ln \mu$  versus  $T^{-2}$  type temperature dependence of the mobility,
- (ii) the  $\ln \mu$  versus  $E^{1/2}$  type field dependence,
- (iii) the temperature dependence of the slope of the  $\ln \mu$  versus  $E^{1/2}$  dependence,
- (iv) the effect of polar functionalities of either transport or matrix molecules and
- (v) the increasing dispersion of time of flight signals at lower temperatures.<sup>1–3</sup>

The key parameters of the formalism are the standard deviation  $\sigma$  of the (Gaussian) distribution of states (DOS), which can be split into a van der Waals component and a polar contribution, and the positional disorder parameter.<sup>10–12</sup> It has been recognized, however, that in experiments the  $\ln \mu$  versus  $E^{1/2}$  type field dependence is obeyed at much lower electric fields than those that Monte Carlo simulations predicted. Recently, major progress concerning this problem was made by introducing correlation among the hopping sites.<sup>13,14</sup> From this, the length scale of the hopping process is extended. It appears that the amended version of the previous hopping formalism provides an adequate basis of experimental analysis.

The aim of this article is to delineate application as well as the limitations for advanced organic transport materials focussing on  $\pi$ -conjugated polymers and discotic liquid crystals. Recent interest was caused by the observation of comparatively large hole mobilities,

Original manuscript received November 23, 1998

▲ IS&T Member

© 1999, IS&T—The Society for Imaging Science and Technology

which are important for the design of organic light emitting diodes. The main questions, which we address, are the role of charge dislocation in a  $\pi$ -conjugated main chain polymer and the effect of static and dynamic disorder in the discotic liquid crystals. We will describe the key observations, delineate both the success as well as the required extensions of the disorder formalism and give an outline of new conceptual approaches which one could envisage.

## Experiment

**Hole Mobility in  $\pi$ -Conjugated Polymers.** Two  $\pi$ -conjugated polymers have been selected for the present study. Methyl-substituted ladder-type poly(para)phenylene (MeLPPP) synthesized by U. Scherf at the Max Planck Institute for Polymer Research in Mainz employing a Suzuki reaction,<sup>15</sup> is a material which exhibits an extraordinary weak disorder, both in liquid and solid solution and in film, manifested by the small inhomogeneously line broadening in both absorption and fluorescence.<sup>16</sup> The reason is the planarization of the skeleton due to covalent bridging. Films, typically 1  $\mu\text{m}$  thick, are prepared by spin-coating onto an indium tin oxide glass slide. Before evaporating a typically 150 nm thick aluminium top contact, the samples were stored for 12 h under reduced pressure of  $10^{-6}$  mbar. Before the experiment one sample—referred to as Sample A—was kept at 150°C under vacuum for at least 4 hr. The widths of the  $S_1 \rightarrow S_0$  0–0 fluorescence bands of Sample B is 375  $\text{cm}^{-1}$  (fwhm) and of Sample A 600  $\text{cm}^{-1}$  (fwhm); the corresponding standard deviations of Gaussian bands are 160  $\text{cm}^{-1}$  and 300  $\text{cm}^{-1}$ . For Sample B there is no indication of defect emission while in Sample A part of the fluorescence is emitted from dimers or aggregates.<sup>16</sup> For comparison, the standard deviation of the  $S_1 \rightarrow S_0$  0–0 absorption band in PPV<sup>17</sup> is 650  $\text{cm}^{-1}$ .

The second material is poly(N-phenylimino-1,4-phenylene-1,2-ethenylene-1,4-(2,5-dioctoxy)-phenylene-1,2-ethenylene-1,4-phenylene) (PAPPV) which was synthesized, by means of a Horner reaction, in the group of Prof. Hörhold at the University of Jena.<sup>18</sup> The PAPPV samples were prepared in the same manner.

Transient photocurrent was generated by an optical parametric oscillator driven at 450 nm (MeLPPP) and 470 nm (PAPPV) using the ITO/polymer interface as a charge generation layer. Typical photocurrent transients of MeLPPP at different applied fields are illustrated in Fig. 1. The signals are normalized to the charge carrier transit time  $t_{tr}$ . After a fast initial spike, the current exhibits a well-established plateau region and then slowly tails off. The TOF signal at  $3 \times 10^5$  V/cm does not show the initial spike due to the limited time resolution of our apparatus. The TOF signals of MeLPPP are nondispersive and feature characteristics of Gaussian charge transport which is in marked contrast to conjugated polymers of the PPV family.<sup>19–21</sup> If the spreading of the tail in the TOF signals is due to thermal diffusion as expected for Gaussian transport, the dispersion  $w$  should decrease by a factor of 2 if the applied voltage is increased by a factor of 5 at a given temperature. It is apparent from Fig. 1 that the transients in MeLPPP do not meet this condition. The shape of the TOF signals is approximately independent of the applied field, i.e., they bear out universality. Therefore, the dispersion cannot be accounted for by thermal diffusion although its presence indicates disorder.

Although the samples show the same characteristics in the shape of the TOF signals, they differ markedly in

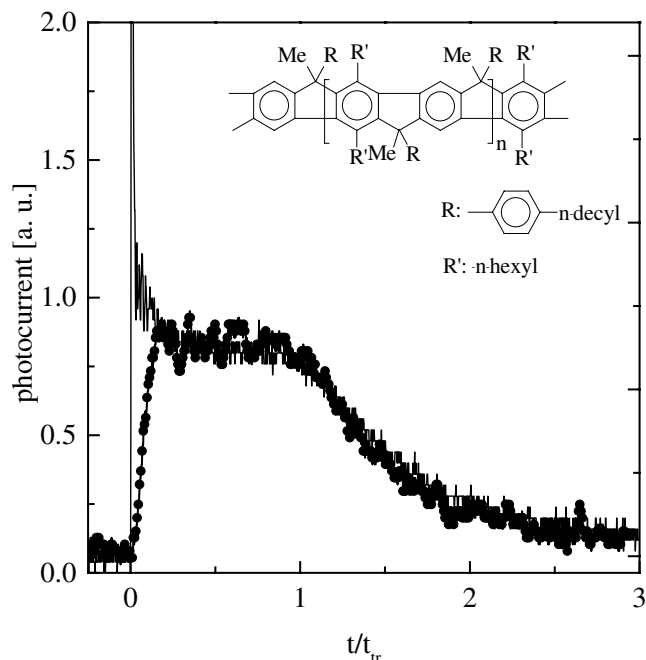


**Figure 1.** Photocurrent transients of MeLPPP normalised to the transit time  $t_{tr}$  at  $T = 243$  K and applied fields of  $E = 6 \times 10^4$  V/cm (solid line) and  $E = 3 \times 10^5$  V/cm (line with solid circles). The inset shows the chemical structure of the MeLPPP.

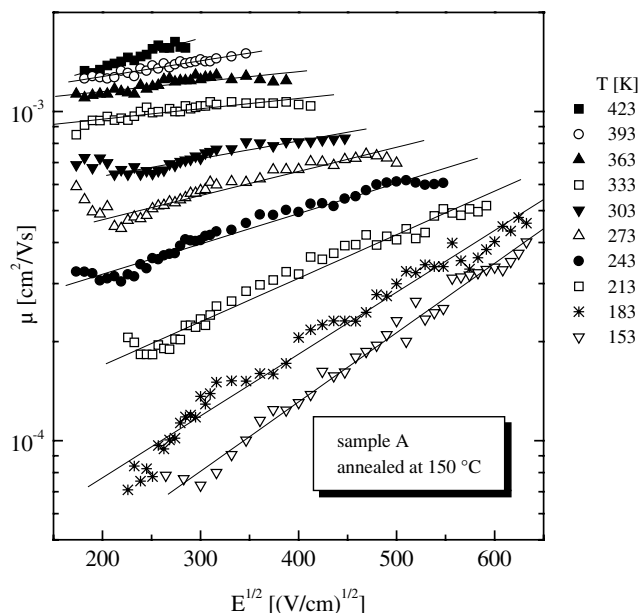


**Figure 2.** Electric field dependence of the mobility  $\mu$  of the MeLPPP Sample A at various temperatures. Data are plotted on a log  $\mu$  versus  $E^{1/2}$  scale.

their temperature and field dependent behaviour. The field dependence of the hole mobility in Sample A ranges from  $7 \times 10^{-5}$   $\text{cm}^2/\text{Vs}$  at 153K to  $1.6 \times 10^{-3}$   $\text{cm}^2/\text{Vs}$  at 423K as shown in Fig. 2. For fields above  $4 \times 10^4$  V/cm, the mobility follows the square root of the electric field which is an ubiquitous feature of molecularly doped polymers or organic glasses. The observed room temperature mobilities of approximately  $1 \times 10^{-3}$   $\text{cm}^2/\text{Vs}$  are orders of magnitude higher than in PPV and its derivatives<sup>19,20</sup> and even higher than in the recently investigated polyfluorene.<sup>22</sup> In Fig. 3, the temperature

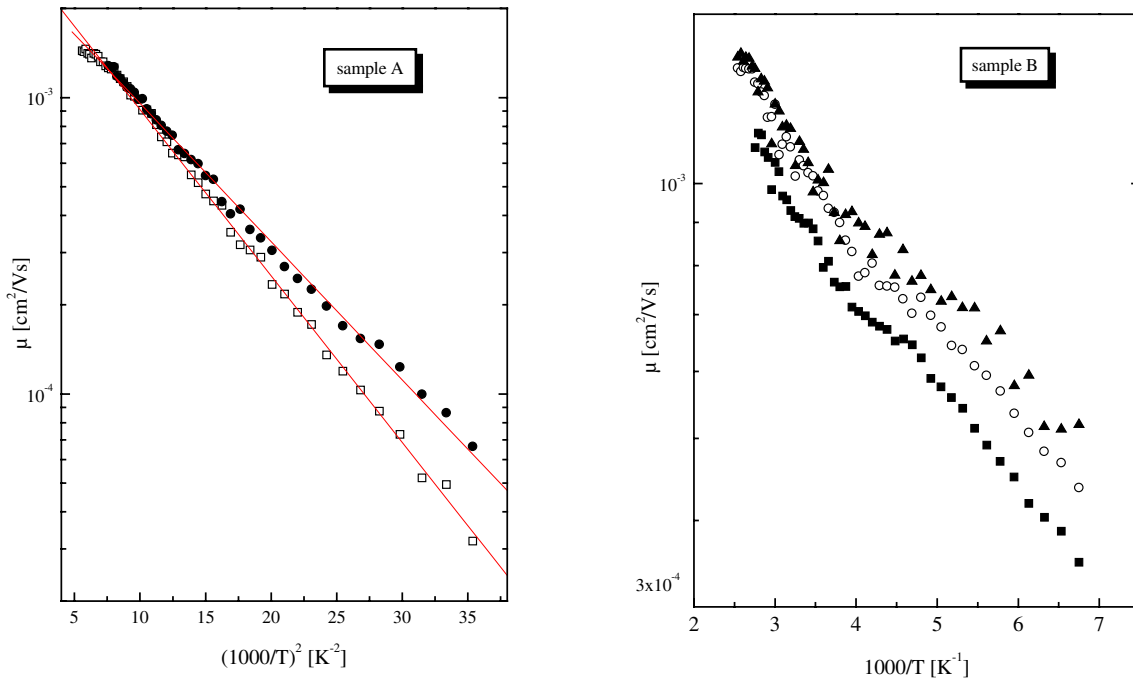


**Figure 3.** The logarithm of the mobility versus  $1/T^2$  for MeLPPP Sample A (left) solid circles:  $E = 1.4 \times 10^5$  V/cm, open squares:  $E = 8 \times 10^4$  V/cm and the Arrhenius plot of the hole mobility of MeLPPP Sample B (right). The symbols refer to  $E = 8 \times 10^4$  V/cm (solid triangles),  $E = 6 \times 10^4$  V/cm (open circles) and  $E = 4 \times 10^4$  V/cm (solid squares).

dependence of the logarithm of the mobility for MeLPPP is plotted versus  $1/T^2$  (left) for Sample A and versus  $1/T$  (right) for Sample B. The weak temperature dependence as well as the negligible electric field dependence of  $\mu$  in Sample B (Fig. 4)<sup>23</sup> are unique and unexpected as far as charge transport of disordered organic solids is concerned. The transport behaviour is similar to that of molecular crystals rather than that of molecularly doped polymers (MDPs). On the other hand the mobility in the MeLPPP film is 2 to 3 orders of magnitude less than in molecular crystals. It cannot be due to trapping, since the low temperature asymptote in the Arrhenius plot translates into an activation energy of only 22 meV ( $E = 4 \times 10^4$  V/cm), which is less than the variance of the distribution of singlet states<sup>24</sup> and at least one order of magnitude less than the activation energies that determine the trap controlled transport of holes in PPV.<sup>19,20</sup> Because arguments that invoke traps are unable to explain the low mobilities, we will discuss these low mobilities as inherent features of MeLPPP.

The temperature dependent mobility (left in Fig. 3) as well as the field dependent mobility of Sample A (Fig. 2) on the other hand, fulfill the relations predicted by the disorder formalism. One can therefore quantify the degree of disorder on the charge transport by calculating the width of the DOS  $\sigma$  according to Eq. 1,  $\mu$  is the mobility,  $\mu_0$  is the mobility at zero field,  $\sigma$  is the energetic disorder parameter (the width of the DOS),  $C$  an empirical constant and  $\Sigma$  is the quantity that describes the positional disorder.<sup>7</sup>

$$\mu = \mu_0 \exp\left[-\left(\frac{2\sigma}{3kT}\right)^2\right] \exp\left[C\left[\left(\frac{\sigma}{kT}\right)^2 - \Sigma^2\right]\sqrt{E}\right] \quad (1)$$

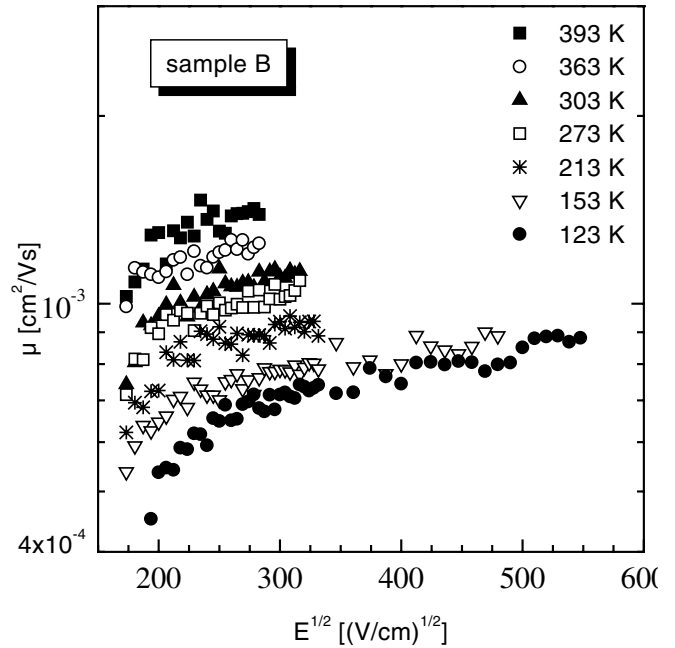


**Figure 4.** The electric field dependence of the hole mobility of MeLPPP Sample B at different temperatures. Data are plotted on a log  $\mu$  versus  $E^{1/2}$  scale.

The zero field mobilities at various temperatures can be extracted from Fig. 2 and plotted versus  $1/T^2$ . The slope of the resulting straight line yields  $\sigma \approx 50$  meV.

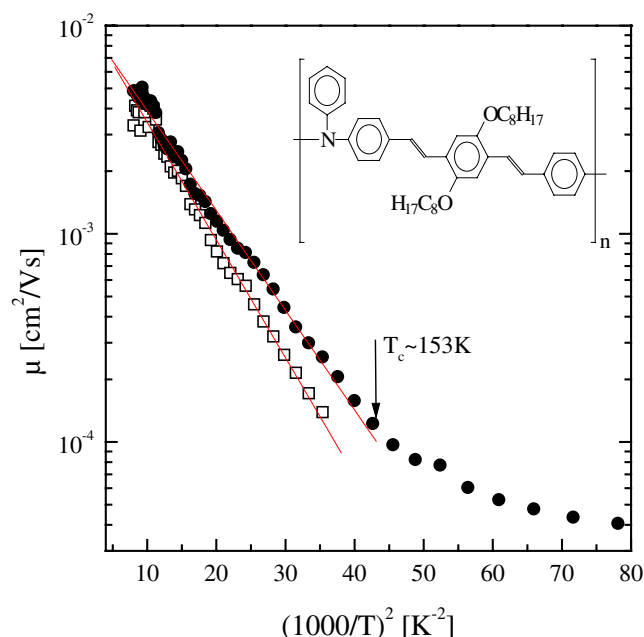


**Figure 5.** The temperature dependence of the mobility  $\mu$  of PAPPV for applied fields of  $E = 7 \times 10^4$  V/cm (solid circles) and  $E = 6.4 \times 10^4$  V/cm (open squares). The  $\log \mu$  is plotted versus  $1/T^2$ . The arrow marks the transition from the nondispersive to the dispersive transport regime. The inset shows the chemical structure of the PAPPV.

Typical values of  $\sigma$  for MDPs<sup>25</sup> are 80 to 100 meV. Although the width of the DOS in MeLPPP is reduced compared with MDPs, the absolute value of the mobility is at least one order of magnitude lower than in MDPs with the highest mobilities, e.g., for the triphenylamine TAPC in polystyrene.<sup>1</sup>

In MeLPPP, the rigid backbone gives rise to improved structural order as compared with PPV-type conjugated polymers. In order to further elucidate the principle of charge transport of the PPV-type polymers we have investigated an amino derivative of PPV (PAPPV). In Fig. 5 the temperature dependence of the mobility is shown. It can be considered as a conventional conjugated polymer with respect to its electronic properties. The broad, structureless absorption and photoluminescence spectra of the PAPPV support this notion. As we have shown recently,<sup>24</sup> the increased disorder in PAPPV leads to a broadening in the tails of the TOF signals as compared with MeLPPP. At temperatures below 153 K the broadening of the tails of the photocurrent transients leads to completely dispersive TOF signals because the charge carriers do not attain their dynamic equilibrium before they reach the electrode. An analysis of the dispersive TOF signals in terms of the Scher-Montroll theory failed as the slopes of the tangents on the current decay in double logarithmic representation do not add up to two.<sup>26</sup> This result is not unexpected since the dispersion in the Scher-Montroll theory originates from the positional disorder in the sample, whereas in conjugated polymers the energetic disorder should be much more important for the charge transport.

An alternative explanation for the disappearance of a clearly indicated transit time is given by MC simulation work where the dispersion was correlated with energetic disorder.<sup>26</sup> At 153 K the initial slope of the PAPPV transient in a double logarithmic scale is  $-0.18$ , which

can be compared with the transients in Ref. 26. The resulting width of the DOS  $\sigma$  is 58 meV. From the field dependence of the mobility in PAPPV, which is similar to that of Sample A of MeLPPP (Fig. 2),<sup>24</sup> we are able to obtain a  $\sigma$  of 52 meV. This value is in reasonable good agreement with the value of 58 meV extracted from the dispersive transient.

MC simulations also provide an estimate of the temperature at which the transition from nondispersive transport to dispersive transport should occur, if the energetic disorder is known:<sup>26</sup>

$$\hat{\sigma}^2 = \left( \frac{\sigma}{kT_c} \right)^2 = 44.8 + 6.7 \log d \quad (2)$$

where  $\sigma$  is the width of the DOS,  $T_c$  the transition temperature and  $d$  the sample thickness in cm. The disorder parameter  $\sigma$  of 52 meV corresponds to a dispersive transport regime below  $T_c = 142$  K. This is only 11 K below the measured transition temperature of 153 K (Fig. 5).

### Discotic Liquid Crystals

Discotic liquid crystals, which form hexagonal columnar mesophases, are of interest for their high hole mobilities. Typical representatives of this class of materials consist of triphenylene cores symmetrically substituted by six aliphatic ethers. Mobilities parallel to the stack axis of  $10^{-4}$  cm<sup>2</sup>/Vs are reported for hexahexyloxytriphenylene (H6T).<sup>27,28</sup> For hexapentyloxytriphenylene (H5T)<sup>29,30</sup> and for hexabutyloxytriphenylene (H4T)<sup>31</sup> values of  $10^{-3}$  cm<sup>2</sup>/Vs and  $10^{-2}$  cm<sup>2</sup>/Vs have been reported, respectively. Perpendicular to the columns, the mobility is two (H5T) to three (H6T) orders of magnitude lower. The relatively high mobilities in the direction of the columns in the liquid crystalline phase have been explained by liquid-like self-healing of structural defects on a time scale faster than hopping of charge carriers. H6T and H5T form the conventional discotic hexagonal ordered phases ( $D_{ho}$ ) featuring a two-dimensional hexagonal intercolumnar order and uncorrelated one-dimensional intracolumnar order. The higher hole mobility in H4T has been attributed to improved order in the discotic hexagonal plastic phase ( $D_{hp}$ ) in which the centers of every disc form a three-dimensional array and the only degree of freedom of the discs is their rotation about the plane axis, their positions in adjacent columns being correlated (see Fig. 6). The existence of the  $D_{hp}$ -phase was first recognized by Glösen and co-workers,<sup>32,33</sup> in H4T and subsequently also found in a few related materials. In all mentioned hexaalkyloxytriphenylenes the hole mobility turned out to be almost field and temperature independent.

In the present work we studied hole transport in discotic liquid crystals based upon the hexaalkyloxytriphenylenes, in which one of the six ether groups is replaced by an ester substituent.<sup>34</sup> This leads to an extended range of the mesophase and suppresses crystallization. This extends the temperature range of transient photoconduction measurements. Four derivatives of H5T, i.e., the ester of pivalic acid (termed pivaloate), the ester of cyclohexane carbonic acid (cyclohexanoate), the ester of 4-cyanobenzoic acid (cyanobenzoate) and the ester of 4-nitrobenzoic acid (nitrobenzoate) and a derivative of H4T, the ester of 4-pentenoic acid (pentenoate), were studied (Fig. 6). Pivaloate and pentenoate show the  $D_{hp}$ -phase within

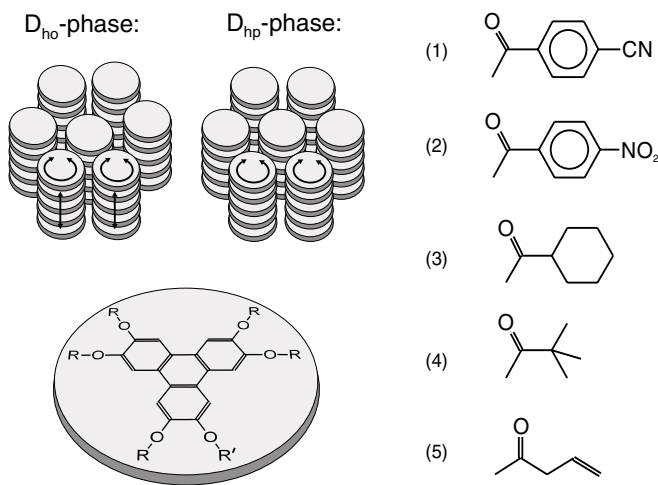


**Figure 6.** At the left side the type of molecular displacements and rotations in the hexagonal ordered phase  $D_{ho}$  and the hexagonal plastic phase  $D_{hp}$  is illustrated. In the bottom the chemical structure of the hexaalkoxytriphenylenes is shown.  $R' = R = C_5H_{11}$  for H5T,  $R' = R = C_4H_9$  for H4T. In the ester substituted compounds  $R'$  is one of the ester substitutes whose chemical structure is shown at the right for (1): cyanobenzoate, (2): nitrobenzoate, (3): cyclohexanoate, (4): pivaloate and (5) pentenoate.

certain temperature ranges. The other materials reveal only the  $D_{ho}$ -phase between the clearing temperature and glass transition.

The starting material for the synthesis is pentaalkoxytriphenylene alcohol synthesized via the biphenyl route as described in Refs. 35 and 36. Subsequently, the esters were prepared by esterifying the triphenylene alcohols with acid chloride as described in Ref. 33. The substances were filled in 30  $\mu\text{m}$  thick sandwich cells at a temperature above the clearing temperature. To orient the discotic substances homeotropically the samples were cooled down from the isotropic phase at a very slow rate, implying an orientation of the columns perpendicular to the substrate.

A standard time-of-flight (TOF) setup was used for measuring the photocurrent transients. The sample was excited with the frequency tripled output of a Nd-YAG laser at 355 nm where the penetration of the light is 1.5  $\mu\text{m}$ . The TOF-signals were non-dispersive. The literature data for hole mobility in H4T have been confirmed.<sup>31</sup> Unlike H4T and H5T, the mobility of the ester derivatives is field dependent, following a  $\ln \mu$  versus  $E^{1/2}$  law, with increasing slope at decreasing temperature. Figure 7 shows the mobility of pentenoate plotted against  $\sqrt{E}$  for several temperatures as an example. The other esters behave similarly.

In contrast with the hexaalkoxytriphenylenes the mobility is temperature dependent. The temperature dependence deviates from the Arrhenius law and rather follows a  $\ln \mu$  versus  $T^{-2}$  relation (Fig. 8) maintaining a constant slope at the glass transition temperature. At the transition between the  $D_{hp}$ -phase and the  $D_{ho}$ -phase a slight decrease of the slope, ( $|\ln d\mu/dT^{-2}|$ ), for pivaloate and pentenoate is noted. It is more pronounced in pivaloate (Fig. 9).

There are some unambiguous signatures of disorder dominated charge carrier hopping as the prevailing transport mechanism<sup>7,9</sup>:

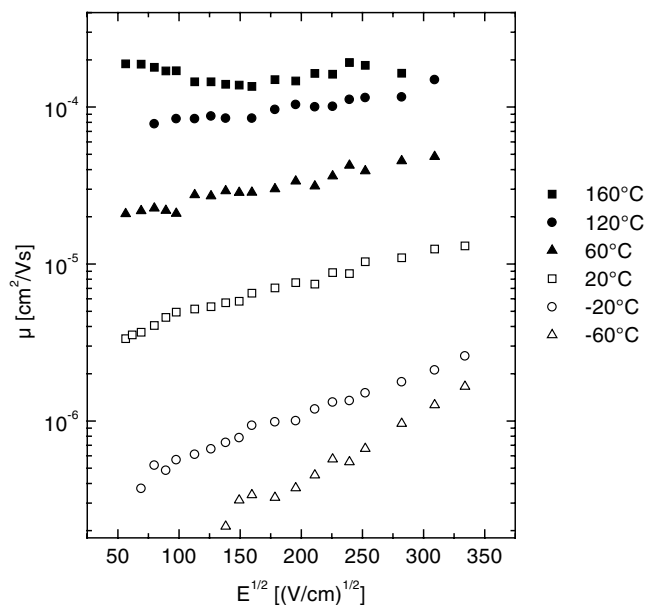


**Figure 7.** Field dependence of the hole mobility in pentenoate at several temperatures.

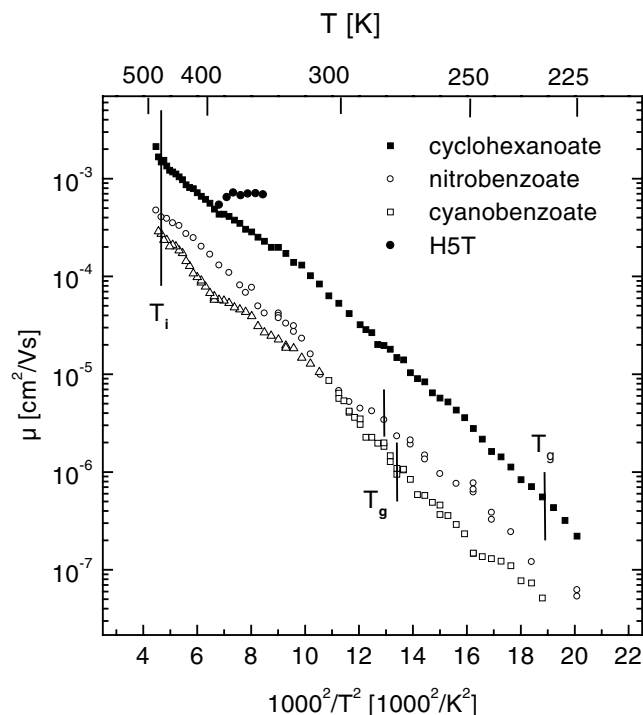


**Figure 8.** Temperature dependence of the hole mobility in cyclohexanoate ( $E = 2.9 \times 10^4$  V/cm), cyanobenzoate ( $E = 10^5$  V/cm) and nitrobenzoate ( $E = 6 \times 10^4$  V/cm) in  $\log \mu$  versus  $T^{-2}$  representation. Clearing temperatures  $T_i$  and glass transition temperatures  $T_g$  are marked. The mobility of H5T is also plotted for comparison.

- (i) The TOF signals of the compounds carrying an ester-substituent broaden upon decreasing temperature.
- (ii) The temperature dependence of their hole mobilities obeys a  $\ln \mu$  versus  $T^{-2}$  law and
- (iii) the field dependence of their mobilities follows a  $\ln \mu$  a  $E^{1/2}$  law, with decreasing slope at increasing temperature.

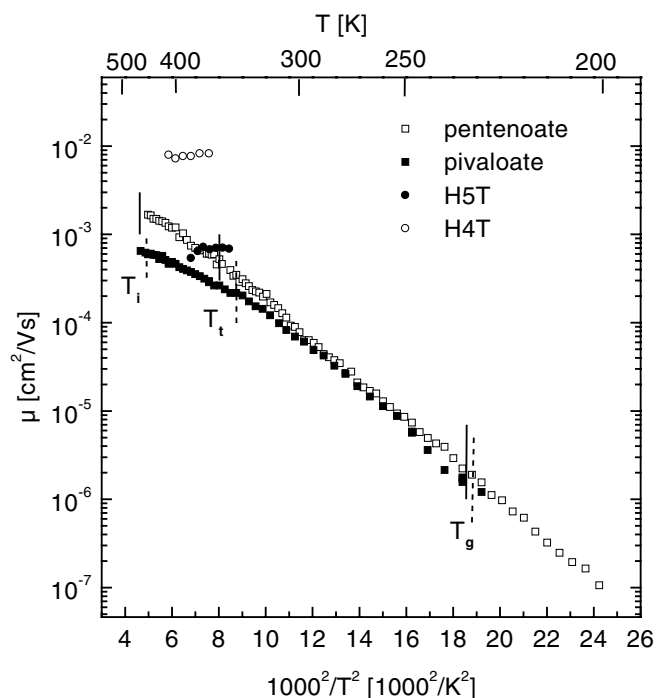


**Figure 9.** Temperature dependence of the hole mobility in pivaloate ( $E = 4.5 \times 10^4$  V/cm) and pentenoate ( $E = 3.2 \times 10^4$  V/cm) in  $\log \mu$  versus  $T^{-2}$  representation. Clearing and glass temperatures  $T_i$  and  $T_g$  and also  $T_c$ , the phase transition temperature between  $D_{ho}$ - and  $D_{hp}$ -phase, are marked by straight lines (pentenoate) or dashed lines (pivaloate). The mobilities of H4T and of H5T are also plotted for comparison.

The  $\mu(E, T)$  dependence of all examined esters is the same as has been observed in molecularly doped polymers, it is in accordance with Eq. 1.

The value of the energetic gaussian width  $\sigma$  is around 100 meV, which is also a typical value for molecularly doped polymers. The lowest values are found in pivaloate and pentenoate, that accordingly also feature the highest mobilities. The highest values of  $\sigma$  are obtained for cyanobenzoate and nitrobenzoate whose group dipole moments are higher. Recall that the group dipole moment of the ester group is  $1.95 D$  and that the moments of the cyano group and of the nitro group attached to a phenyl ring are  $4.18 D$  and  $4.22 D$ , respectively. The effect is well documented in the literature on molecularly doped polymers and molecular glasses.<sup>10–12,37,38</sup> It has been ascribed to the increase of the fluctuation of the random electric fields in the vicinity of positionally disordered molecules carrying dipole moments. A summary of the energetic as well as the positional disorder parameters is given in Table I.

## Discussion

It is apparent that certain aspects of charge carrier motion in  $\pi$ -conjugated polymers and discotic liquid crystals are in accordance with the predictions of the disorder formalism for Gaussian shaped DOS while others require conceptual modifications. The successful interpretation of the hole mobilities in discotic liquid crystals carrying ester substituents in terms of the disorder formalism implies the absence of coherence effects. It is obvious that it is sufficient to consider nearest neighbour hopping only. Apparently, the variance of the intermo-

**TABLE I.** List of the Energetic Order Parameters  $\sigma$  and Positional Order Parameters  $\Sigma$  of the Hopping Sites Derived from the Analysis of  $\mu(E, T)$  Data.

Compound	$\sigma$ (meV)	$\Sigma$
Pivaloate	84	1.8
Pentenoate	104	1.8
Cyclohexanoate	108	2.5
Cyanobenzoate	124	2.6
Nitrobenzoate	127	3.0

lecular spacing and, in the hexagonal plastic phase, even the rotation of molecules carrying polar substituents is sufficient to destroy any possible coherence effects and to localize a charge carrier. Extrapolating the linear portion of  $\ln \mu$  versus  $T^{-2}$  plots towards very high temperature yields values of  $\mu_0$  ranging from  $0.03 \text{ cm}^2/\text{Vs}$  (pivaloate, pentenoate and cyclohexanoate) to around  $5 \times 10^{-3} \text{ cm}^2/\text{Vs}$  which is less than the value for molecular crystals. At higher temperatures the slope of  $\ln \mu$  versus  $T^{-2}$  plots tends to decrease. This effect is most pronounced with pivaloate at the transition from the hexagonal plastic  $D_{hp}$ -phase to the  $D_{ho}$ -phase. A similar effect has been found with molecularly doped polymers and molecular glasses above the glass transition temperature. It has been ascribed to the onset of dynamic disorder<sup>39</sup> yielding smaller values of  $\mu$  as expected on the premise of a constant static disorder potential.

It is remarkable that the hole mobilities in symmetric H4T and H5T are temperature independent while those of the asymmetric esters follow a  $\ln \mu$  versus  $T^{-2}$  dependence. Further, the mobility of H4T more or less agrees with the  $1/T \rightarrow 0$  intercept of the  $\ln \mu$  versus  $1/T^{-2}$  plot of pentenoate, i.e., of derivatized H4T. This suggests that the main reason of the disorder is the presence of random potential fluctuations caused by polar functionality. This is confirmed by the variation of the energetic order parameter  $\sigma$  with the group dipole moments and the reduced disorder evident from the temperature and field independence of the hole mobility of unsubstituted H4T. On the other hand the rather low and temperature independent value of  $\mu$  in the discotic phase of unsubstituted H4T as compared with molecular crystals, indicates that the limiting process for non-activated hopping is likely to be associated with the rotation of the disc-like molecules that prevent optimum electronic overlap rather than due to energetic disorder.

As far as conjugated polymers are concerned the disorder formalism provides an adequate description of the hole mobility in PAPPV and the MeLPPP after heat treatment which may introduce aggregates that act as physical traps. However, trap-free and only weakly disordered MeLPPP behave differently as far as the temperature and the field dependence is concerned. In order to explain the low mobility of MeLPPP, arguments have to be invoked which are yet not included in the disorder model. Charge transport in MDPs occurs by transfer of charges from molecule to molecule, each being different in energy due to disorder. This is reflected in the dependence of charge transfer on temperature and electric field. In these cases the mean free path of the carrier is equal to the intermolecular distance. For conjugated polymers, that may not necessarily be true. A polymer like MeLPPP consists of arrays of subunits which are disordered and separated by topological defects, these segments being more or less electronically decoupled. The length of the segments is subjected to a statistical

distribution resulting in inhomogeneous broadening of the absorption and fluorescence spectra. The effective conjugation length for MeLPPP is  $6.5 \pm 0.5$  nm, equivalent to  $14.5 \pm 1.5$  phenylene units.<sup>40</sup> Charge transport in conjugated polymers occurs both by migration between the segments of the same chain (on-chain transport) and by hopping between adjacent chains (inter-chain transport).

A weak temperature dependence of the mobility requires a low activation energy of rate-limiting carrier jumps. For a system of point-like hopping sites this implies weak energy and/or strong positional disorder. Under the condition  $\sigma < kT$  the mobility must be practically independent of the temperature and reveal a weak field dependence within the whole range of variation of these two parameters. However, the above condition is not fulfilled even for weakly disordered conjugated polymers such as MeLPPP especially at lower temperatures where anomalously weak  $T$ - and  $F$ -dependencies of the mobility are still observed. A strong positional disorder implies a broad distribution of inter-site distances that is possible only in a diluted hopping system. Making a jump over the distance  $\Delta x$  along the field  $F$  a carrier gains the electrostatic energy  $\Delta E = eF\Delta x$ . If this energy is higher than both  $kT$  and  $\sigma$ , carriers will jump mostly along the field direction and such jumps will require no activation. Under these conditions both the field and temperature dependences of the transit time must saturate and longest non-activated jumps along the field direction will play a role of rate-limiting steps. In a hopping system with both positional and energy disorder, the regime of  $T$ -independent mobility sets on at a sufficiently strong field:  $F > \sigma/e\Delta x$ . For conjugated polymers with typical inter-site distance of 0.6 nm and  $\sigma$  ranging from 50 to 100 meV this estimate yields  $F$  ranging from  $8 \times 10^5$  to  $1.5 \times 10^6$  V/cm. This is at least one order of magnitude higher than the experimentally observed onset of the regime of weak field and temperature dependence of the mobility in MeLPPP. Therefore the traditional version of the disorder model cannot account for the lack of  $F$ - and  $T$ -dependence of the mobility in weakly disordered conjugated polymers.

These materials consist of arrays of coupled subunits (conjugated segments) which are positionally and orientationally disordered. Conjugated segments, that belong to the same polymer chain, are separated by topological defects. Charge carriers occupy extended states and are therefore mobile within segments while charge transfer between different segments occurs via tunneling jumps. The length of segments ranges from 5 to 10 nm in different materials that is much longer than the inter-segmental distance of typically 0.6 nm. Under these conditions, carriers may cross the longest part of the total distance moving in the conduction band of conjugated segments and make much fewer inter-segmental tunneling jumps compared to what is predicted by the model of a random network of point-like hopping sites.

The variation of carrier electrostatic energy in the field of  $10^5$  V/cm on the length of 6 nm is 0.06 eV, which is larger than the thermal energy of 0.025 eV at the room temperature. Under these circumstances carriers are localized within a field-induced potential well close to the low energy ends of segments independent of the point at which the carrier has entered the segments and carriers gain much more electrostatic energy by traveling along a segment than that which they can gain by making a jump between sites. This is essentially equivalent

to the field-induced positional disorder. On the one hand, field-assisted localization makes inter-segmental jumps of carriers against the field direction difficult even at moderate fields. Under such conditions carrier jumps from dead ends of segments along the field direction will be the rate-limiting steps. On the other hand, one may expect a much larger localization radius for tunneling jumps within a segment compared to that for inter-segmental jumps. This can strongly enhance long carrier jumps in the forward direction and suppress the effect of energetic disorder. The intra-segmental contribution to the gain of electrostatic energy makes rate-limiting carrier tunneling jumps easier onto shallower segments along the field direction and effectively reduces the activation energy of the hopping drift mobility. Moreover, if the intra-segmental gain of energy at a given external field exceeds the width of the DOS, carrier hopping may need no further thermal activation and both the field and the temperature dependencies of the mobility practically vanish. Quantitative description of charge transport in disordered hopping systems with finite size of hopping sites will be given in a future work of the authors including consideration of the orientational disorder caused by random orientations of conjugated segments.  $\blacktriangle$

**Acknowledgement.** It is a pleasure to acknowledge the contribution of H. H. Hörhold, A. Kettner, J. Kopitzke and J. H. Wendorff. This work was supported by the Deutsche Forschungsgemeinschaft (Sonderforschungsbereich 383 and 436 Rus 113/9314).

## References

1. P. M. Borsenberger, L. Pautmeier and H. Bässler, *J. Chem. Phys.* **94**, 5447 (1991).
2. P. M. Borsenberger and D. S. Weiss, *Organic Photoreceptors for Imaging Systems*, Marcel Dekker, New York, 1992.
3. M. A. Abkowitz, H. Bässler and M. Stolka, *Phil. Mag. B* **63**, 201 (1991).
4. R. I. Personov, in *Spectroscopy and excitation dynamics of condensed molecular systems*, V. M. Argranovitch and R. M. Hochstrasser, Eds., North Holland, Amsterdam, 1983, p. 555.
5. R. Eiermann, G. M. Parkinson, H. Bässler, and J. M. Thomas, *J. Phys. Chem.* **86**, 313 (1982).
6. A. Kadashchuk, N. Ostapenko, V. Zaiko, and S. Nèspùrek, *Chem. Phys.* **234**, 285 (1998).
7. H. Bässler, *Phys. stat. sol. (b)* **15**, 175 (1993).
8. B. Movaghar, M. Grünwald, B. Ries, H. Bässler, and D. Würtz, *Phys. Rev. B* **33**, 5545 (1986).
9. H. Bässler, in *Disorder Effects on Relaxational Processes*, R. Richert and A. Blumen, Eds., Springer-Verlag, Berlin, Heidelberg 1994, p. 485.
10. P. M. Borsenberger and J. J. Fitzgerald, *J. Phys. Chem.* **97**, 4815 (1993).
11. P. M. Borsenberger and H. Bässler, *J. Chem. Phys.* **95**, 5327 (1991).
12. P. M. Borsenberger, W. T. Gruenbaum, E. H. Magin, and L. J. Sorriero, *Chem. Phys.* **195**, 435 (1995).
13. Yu. N. Gartstein and E. M. Conwell, *Chem. Phys.* **245**, 351 (1995).
14. D. H. Dunlap, P. E. Parris and V. M. Kenkre, *Phys. Rev. Lett.* **77**, 542 (1996).
15. U. Scherf, A. Bohnen and K. Müllen, *Makromol. Chem.* **193**, 1127 (1992).
16. R. F. Mahrt, T. Pauck, U. Lemmer, U. Siegner, M. Hopmeier, R. Henning, H. Bässler, E. O. Göbel, P. Haring Bolivar, G. Wegmann, H. Kurz, U. Scherf, and K. Müllen, *Phys. Rev. B* **54**, 1759 (1996).
17. S. Heun, R. F. Mahrt, A. Greiner, U. Lemmer, H. Bässler, D. A. Halliday, D. D. C. Bradley, P. L. Burns, and A. B. Holmes, *J. Phys. Condens. Matter* **5**, 247 (1993).
18. H. Rost, A. Teuschel, S. Pfeiffer, and H. H. Hörhold, *Synth. Met.* **84**, 269 (1997).
19. H. Meyer, D. Haarer, H. Naarmann, and H. H. Hörhold, *Phys. Rev. B* **52**, 2587 (1995).
20. E. Lebedev, Th. Dittrich, V. Petrova-Koch, S. Karg, and W. Brütting, *Appl. Phys. Lett.* **71**, 2686 (1997).
21. P. W. M. Blom and M. C. J. M. Vissenberg, *Phys. Rev. Lett.* **80**, 3819 (1998).

22. M. Redecker, D. D. C. Bradley, M. Inbasekaran, and E. P. Woo, *Appl. Phys. Lett.* **73**, 1565 (1998).
23. D. Hertel, U. Scherf and H. Bässler, *Adv. Mat.* **10**, 1119 (1998).
24. D. Hertel, U. Scherf, H. H. Hörhold, and H. Bässler, *J. Chem. Phys.* **110** (1999).
25. P. M. Borsenberger, E. H. Magin, M. Van der Auweraer, and F. C. De Schryver, *Phys. stat. sol. (a)* **140**, 9 (1993).
26. P. M. Borsenberger, L. Pautmeier and H. Bässler, *Phys. Rev. B* **46**, 12145 (1992).
27. N. Boden, R. J. Bushby, J. Clements, B. Movaghar, K. J. Donovan, and T. Kreouzis, *Phys. Rev. B* **52**, 13274 (1995).
28. N. Boden, R. J. Bushby, J. Clements, K. Donovan, B. Movaghar, and T. Kreouzis, *Phys. Rev. B* **58**, 3063 (1998).
29. D. Adam, F. Closs, T. Frey, D. Funhoff, D. Haarer, H. Ringsdorf, P. Schumacher, and H. Siemensmeyer, *Phys. Rev. Lett.* **70**, 457 (1993).
30. D. Adam, D. Haarer, F. Closs, T. Frey, D. Funhoff, K. Siemensmeyer, P. Schumacher, and H. Ringsdorf, *Ber. Bunsenges. Phys. Chem.* **97**, 1366 (1993).
31. J. Simmerer, *Adv. Mat.* **8**, 815 (1996).
32. B. Glüsen, W. Heitz, A. Kettner, and J. H. Wendorff, *Liq. Cryst.* **20**, 627 (1996).
33. B. Glüsen, A. Kettner and J. H. Wendorff, *Mol. Cryst. Liq. Cryst.* **303**, 115 (1997).
34. A. Ochse, A. Kettner, J. Kopitzke, J. H. Wendorff, and H. Bässler, *Phys. Chem. Chem. Phys.* **1**, 1757 (1999).
35. N. Boden, R. C. Borner, R. J. Bushby, and A. N. Cammidge, *J. Chem. Soc., Chem. Commun.* **1994**, 465 (1994).
36. P. Henderson, H. Ringsdorf and P. Schumacher, *Liq. Cryst.* **18**, 191 (1995).
37. P. M. Borsenberger and M. B. O'Regan, *Chem. Phys.* **200**, 257 (1995).
38. P. M. Borsenberger, E. H. Magin and J. Shi, *Physica B* **217**, 212 (1996).
39. P. M. Borsenberger, L. Pautmeier and H. Bässler, *J. Chem. Phys.* **95**, 1258 (1991).
40. J. Grimme, M. Kreyenschmidt, F. Uckert, K. Müllen, and U. Scherf, *Adv. Mat.* **7**, 292 (1995).